Scientific Reports

https://doi.org/10.1038/s41598-026-40874-z

Article in Press

Mechanical and durability assessment of marble dust–fiber concrete supported by ML prediction

Received: 2 December 2025

Accepted: 16 February 2026

Published online: 21 February 2026

Cite this article as: Sai A.N., Sakthivel M., Arunvivek G.K. *et al.* Mechanical and durability assessment of marble dust–fiber concrete supported by ML prediction. *Sci Rep* (2026). https://doi.org/10.1038/s41598-026-40874-z

Ayinala Naga Sai, M. Sakthivel, G. K. Arunvivek, Pramod Kumar, R. Dharmaraj & Regasa Yadeta Sembeta

Mechanical and Durability Assessment of Marble Dust–Fiber Concrete Supported by ML Prediction

Ayinala Naga Sai[1], M. Sakthivel[2], G. K. Arunvivek[3], Pramod Kumar[4], R. Dharmaraj[5], Regasa Yadeta Sembeta[6]*

[1]Department of Civil Engineering, Aditya University, Surampalem, Andhra Pradesh, India.

[2]Department of Civil Engineering, Kongunadu College of Engineering and Technology, Trichy, Tamil Nadu, India

[3]Department of Civil Engineering, Mohan Babu University, Tirupati 517102, India.

[4]Department of Civil Engineering, Graphic Era (Deemed to be University), Dehradun, Uttarakhand, India.

[5]Department of Civil Engineering, KPR Institute of Engineering and Technology, Coimbatore, Tamil Nadu, India

[6]Department of Civil Engineering, College of Engineering and Technology, Mattu University, Metu, Ethiopia- 318

*Corresponding author: yadetaregasa@gmail.com

Abstract: This research investigates the need for sustainable, high-performance concrete by blending waste marble dust (MD) with recycled polypropylene fiber (PF) to reduce cement consumption and enhance concrete's mechanical properties. An extensive experimental Programme was designed: 25 mix designs with varying MD levels (0-20%) and PF dosages (0-1.0%) were performed, and the experimental study was further aided by ML models for predicting and improving concrete properties. Fresh, durability and mechanical properties, with slump, density, compressive strength, flexural strength, split tensile strength, water absorption, permeability, and acid resistance, were measured. The compressive strength increased from 51.62 MPa for the control mix to 57.7 MPa at 10% MD replacement and 1.0% PF addition. However, mixes

containing 10% MD with 0.6% to 0.8% PF exhibited comparable compressive strength while demonstrating better overall performance in terms of strength, durability, and workability. The split tensile strength increased from 3.236 MPa for the control mix (A0) to the maximum value of 4.249 MPa at 10% MD and 0.8% PF, which is an improvement of about 31%, and similarly, the flexural strength increased by 25% (to 5.54 MPa) compared to the conventional mix. Durability showed considerable improvements, with the amount of water absorbed decreasing from 3.42% to 2.84% and a 30% reduction in permeability (from 9.42 × 10-12 to 6.64 × 10-12 m/s). The ANN models yielded R^2 values> 0.95 and thus demonstrated high predictive accuracy. One of the novel aspects of this study is the interaction among the integration of waste MD and secondhand PF, machine learning-based prediction and optimization, which enable the precise determination of the optimal mix proportions with respect to strength, durability, and sustainability, surpassing traditional empirical design methodologies.

Keywords: Marble Dust; PF Reinforcement; Mechanical and Durability Performance; ML Optimization; Eco-Efficient Concrete Mix Design.

1. Introduction

The global construction industry faces growing environmental pressures associated with the overconsumption of cement and the resulting waste. Cement production is the main cause of the largest share of carbon dioxide emissions worldwide at about 8 %, largely because of limestone calcination and associated energy-intensive processes in clinker production [1]. To mitigate these effects, research has explored the use of supplementary materials, such as fly ash, silica fume, and marble dust (MD), which can partially replace the cement used to decrease the carbon footprint of concrete [2]. However, the large-scale use of MD is restricted, despite its high calcium carbonate content and potential as a micro-filler. Previous revisions have demonstrated the use of MD to improve particle packing and

enhance early-age strength. However, they found that excessive replacement, starting from 15% onwards, leads to strength loss due to binder dilution and increased water demand [3, 4]. Similarly, workability and segregation related problems limit its effective use; thus, the need evolved for an optimized mix design [5, 6].

At the same time, the accumulation of non-biodegradable plastic (especially polypropylene) significantly helps the ecological environment. Global PP production exceeds 80 million tonnes per year, representing a significant share of long-term environmental pollution [7, 8]. The reuse of this waste in the form of synthetic fibers in concrete is a sustainable strategy to optimize the mechanical and durability performance. Polypropylene fibres (PF) help control crack propagation, enhance tensile and flexural strength, and improve impact strength by redistributing stress. However, the high fibre content (>1.0%) has reduced workability, increased air voids, and caused compaction difficulties [9]. Moreover, the combined effect of MD and PF regarding fresh, mechanical and durability behaviour has been inadequately investigated, and few studies have optimized the interaction of the two in a consolidated perspective [2].

Recent progress in machine learning (ML) has eliminated the usage of empirical/trial-based design in concrete mix optimization [10, 11]. Algorithms like ANN, SVR and RF models can encapsulate complex nonlinear relationships between mix parameters (i.e. cement, water-binder ratio, fibre and filler content) and resultant properties (i.e. strength and durability) [10, 12]. By capitalizing on these tools, the current research combines ML-enabled predictive modelling with experimental evaluation of MD (0-20% w/w) and PF (0-1% w/w) combinations, opening the door to optimal proportions for optimal performance and sustainability, and the experimental data-driven route for the development of the next generation of eco-efficient concrete [13].

Previous studies on sustainable concrete have separately demonstrated the benefits of MD as a fine filler and of PF as a tensile-strength enhancer.

MD, being rich in calcium carbonate, increases the packing density, refines the interfacial (ITZ), while increasing early age compressive strength by partial cement replacements up to approximately 10-15% of cement [14, 15]. However, beyond this limit, excessive MD leads to excessive water demand and binder dilution with consequent reduced strength and durability [16, 17]. Similarly, PF inclusion in the range of 0.4-0.8% by volume has an effective range to bridge cracks and provide improved tensile and flexural strength, also enhances toughness, but when higher dosages are used (greater than 1.0%), fibers tend to agglomerate and cause reduced workability, air voids and poor compaction [16], [17].

Despite these improvements, in the past, these two waste modifiers have been considered separately with little quantitative optimization of their co-action towards the fresh, mechanical, and durability characteristics. Moreover, machine learning-based prediction/optimization frameworks correlated between MD and PF contents and measured performance parameters have been found to be underexplored in the existing literature set. In the present study a systematic and Integrated Artificial Intelligence (I.A.I) based experimental Programme is developed to determine the combined and synergistic influence of the MD (0%, 5%, 10%, 15%, 20%) and PF (0%, 0.4%, 0.6%, 0.8%, 1.0%) in a comprehensive matrix of mixes designated as; A0 - A4, B0 - B4, C0 - C4, D0 - D4 and E0 - E4. The investigation involves fresh properties (slump, compaction factor, and fresh density) and hardened properties (mechanical and durability performance). Mechanical evaluation includes compressive, split tensile, and flexural strengths, while durability tests include water absorption, acid resistance, and water permeability. To go beyond normal empirical interpretation, machine learning models, RF, SVR, and ANN are used to forecast and optimize strength and durability results as a function of mix composition. In contrast to previous research efforts that used MD or PF separately and/or relied solely on machine learning for strength estimation, this research presents an integrated experimental-computational framework that

leverages both waste materials and advanced machine learning algorithms. This methodology enables the systematic optimization of fresh, mechanical and durability attributes, while simultaneously decreasing the experimental uncertainty and having a lower environmental footprint.

2 Materials

OPC grade 53, as per IS 122693 [58], was used as the primary binder. The cement had a specific gravity of 3.15, an initial setting time of 32 minutes and a final setting time of 210 minutes. Its Blaine fineness was calculated to be around 320 - 350 m^2 kg, meaning it is a relatively fine particle size, favorable to the hydration kinetics. OPC grade 53 is favored widely for high-strength applications due to its high early reactivity, which helps the formation of calcium siliceous hydride (C-S-H) gel or early age strength of concrete [16, 18]. The mineralogical constitution of the material is mainly comprised of C3S and C2S, both of which are the direct factors in developing strength [19]. Natural river sand conforming to Zone 2 of IS 383:2016 was used as a fine aggregate. This sand exhibited fineness (2.65) and specific gravity (2.60), indicating a medium gradation and suitability for the fabrication of a dense matrix, such as a mortar prosthesis. The silt content was less than 2 % which minimized any interference with the hydration of cement. Well-graded fine aggregates increase workability/cohesion and decrease water demand by increasing the particle-packed density [20, 21].

Crushed granite, a coarse aggregate with a nominal size of 20 mm, was used in accordance with IS 383 [59]. The aggregate showed a specific gravity of 2.70, a water absorption rate of 0.5-0.8%, and an impact value of less than 22%, indicating good strength and durability. The angular nature of the aggregate helps increase the interlock and load-transfer mechanisms of the hardened concrete matrix [22, 23]. The course/fine aggregate ratio has been set at 60:40, providing adequate compressive resistance while maintaining a workable rheology. MD was gained from the resident marble

quarrying industry in Chennai as a waste by-product. This filler effect contributes to densification of the interfacial transition zone (ITZ), the formation of greater amounts of hydration products, and thus to the development of mechanical strength and a reduction in permeability [24, 25].

Figure 1. Materials Used (a) River Sand, (b) Coarse Aggregates, (c) Cement mortar, (d) Cube

The recycled PF had tensile strengths above 400 MPa, moduli of elasticity of 3 - 5 GPa and negligible water absorption levels. Appropriate fiber dispersion is very important to achieve performance benefits [26, 27]. The physical appearance and features of the constituent materials used in the experimental program are shown in Figure 1. Potable tap water, free from organic impurities, as per IS 456 [60] standards, was used for mixing and curing. A high-range water-reducing intermixture based on PCE was

used at a dosage of 0.6% of the cement weight. The use of PCE admixtures improves slump retention and reduces bleeding tendency, especially in fibre-reinforced mixes where internal friction is high [28, 29]. The chemical and physical characteristics of the constituent materials used for this education are summarized in Table 1.

Table 1. Physical and Chemical Properties of Materials Used in the Experimental Program

Material	Physical Properties	Value	Chemical Composition (Major Oxides %)
OPC53 Grade	Specific gravity	3.15	CaO 63.2 SiO_2 21.4 Al_2O_3 5.3 Fe_2O_3 3.4 MgO 1.8 SO_3 2.4
	Blaine fineness (m^2/kg)	335	
	Initial / Final setting time (min)	32 / 210	
	Colour	Grey	
Fine Aggregate (Natural River Sand, Zone II)	Specific gravity	2.60	SiO_2 95.3 Al_2O_3 2.1 Fe_2O_3 0.6; CaO 0.5 MgO 0.4
	Fineness modulus	2.65	
	Water absorption (%)	1.2	
	Bulk density (kg/m^3)	1650	
Coarse Aggregate (Crushed Granite, 20 mm)	Specific gravity	2.70	SiO_2 68.1 Al_2O_3 15.5 Fe_2O_3 3.2 CaO 5.9 MgO 2.3
	Water absorption (%)	0.65	
	Impact value (%)	< 22	
	Bulk density	1500	

	(kg/m³)			
Marble Dust (Industrial Waste Filler)	Specific gravity	2.65	$CaCO_3$	85–98
	Particle size (μm)	< 90	MgO	1.5
	Colour	White	SiO_2	1.2
	Moisture content (%)	< 1	Fe_2O_3	0.3
			Loss on ignition	38–42
Polypropylene Fibre (Recycled)	Fibre length (mm)	12	C_3H_6 (Polymer chain)	
	Tensile strength (MPa)	> 400		
	Elastic modulus (GPa)	4		
	Specific gravity	0.91		
	Water absorption (%)	Nil		
Superplasticizer (PCE-Based)	Specific gravity	1.10	Main constituents: Polycarboxylate ether (–COOH functional groups)	
	Recommended dosage (% of binder)	0.6		

3. Methodology

This study uses an integrated experimental and machine Learning-based approach to evaluate and optimize the performance of concrete modified with MD and PF. The methodology includes the formulation of mix designs, preparation of specimens and testing of fresh, mechanical and durability properties, followed by data-driven prediction and optimization using artificial neural network, support vector regression, and random forest models. The general workflow used in this investigation is shown in Figure 2.

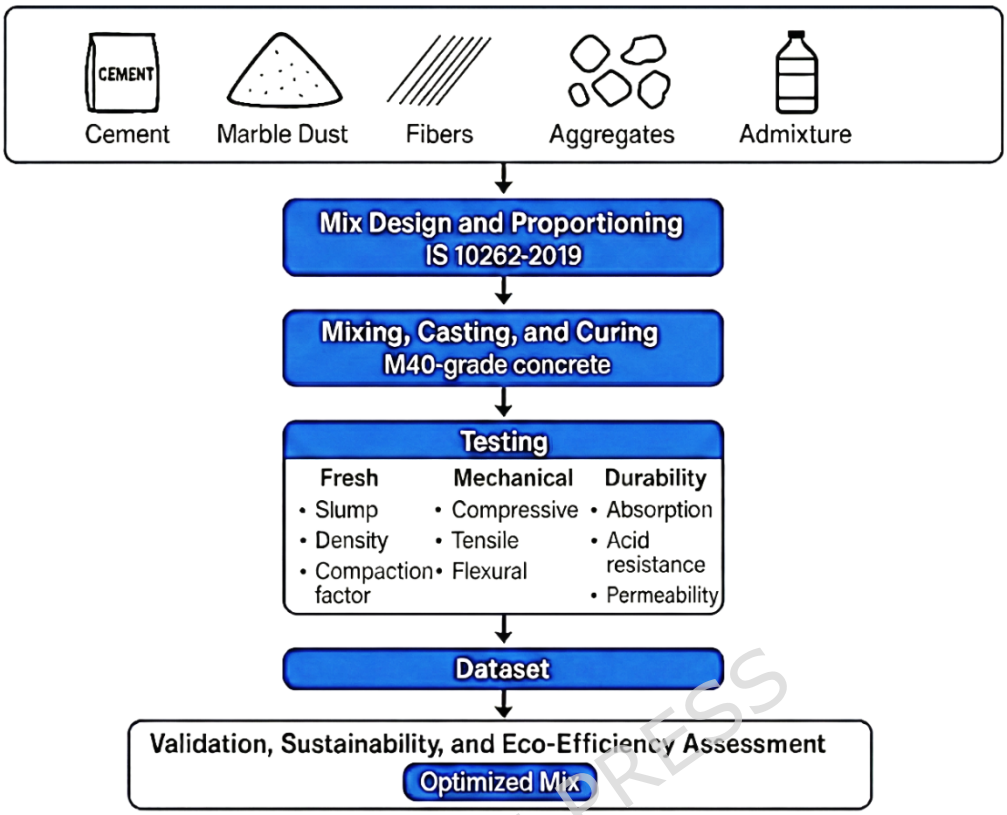

Figure 2. Experimental Workflow for AI-Integrated Evaluation of MD and PF Concrete

The concrete used in this investigation was formulated to meet the M40 grade limit as specified in IS:10262 [61] and IS:456 [60]. The required mean compressive strength was determined from the standard deviation and the margin of safety. A w/c ratio of 0.40 was used according to durability and strength requirements. Cement replacement was performed using MD at predetermined levels of 0%, 5%, 10%, 15%, and 20%. PF were added at 0.0%, 0.4%, 0.6%, 0.8%, and 1.0% volume. The proportions of the mixtures, identified by the ID number from A0 to E4, and the respective replacement levels of MD and dosages of PF are listed in Table 2. Although cement was partially replaced by MD on a mass basis and fibres were incorporated on a volumetric basis, the aggregate quantity was kept constant, with only minor adjustments to the weight to maintain the concrete mixtures' volumetric consistency.

Table 2. Mix Proportion Details of MD and PF-Based Concrete (M40 Grade)

Mix ID	MD (%)	PF (vol %)	Cement (kg/m³)	Marble dust (kg/m³)	Water (kg/m³)	SP (kg/m³)	Fiber (kg/m³)	Aggregates total (kg/m³)	Coarse (60%)	Fine (40%)
A0	0	0.0	400.00	0.00	160.00	2.40	0.000	1837.60	1102.56	735.04
A1	0	0.4	400.00	0.00	160.00	2.40	3.640	1833.96	1100.38	733.58
A2	0	0.6	400.00	0.00	160.00	2.40	5.460	1832.14	1099.28	732.86
A3	0	0.8	400.00	0.00	160.00	2.40	7.280	1830.28	1098.17	732.11
A4	0	1.0	400.00	0.00	160.00	2.40	9.100	1828.40	1097.04	731.36
B0	5	0.0	380.00	20.00	160.00	2.40	0.000	1837.60	1102.56	735.04
B1	5	0.4	380.00	20.00	160.00	2.40	3.640	1833.96	1100.38	733.58
B2	5	0.6	380.00	20.00	160.00	2.40	5.460	1832.14	1099.28	732.86
B3	5	0.8	380.00	20.00	160.00	2.40	7.280	1830.28	1098.17	732.11
B4	5	1.0	380.00	20.00	160.00	2.40	9.100	1828.40	1097.04	731.36
C0	10	0.0	360.00	40.00	160.00	2.40	0.000	1837.60	1102.56	735.04
C1	10	0.4	360.00	40.00	160.00	2.40	3.640	1833.96	1100.38	733.58
C2	10	0.6	360.00	40.00	160.00	2.40	5.460	1832.1	1099.2	732.

								4	8	86
C3	10	0.8	360.00	40.00	160.00	2.40	7.280	1830.28	1098.17	732.11
C4	10	1.0	360.00	40.00	160.00	2.40	9.100	1828.40	1097.04	731.36
D0	15	0.0	340.00	60.00	160.00	2.40	0.000	1837.60	1102.56	735.04
D1	15	0.4	340.00	60.00	160.00	2.40	3.640	1833.96	1100.38	733.58
D2	15	0.6	340.00	60.00	160.00	2.40	5.460	1832.14	1099.28	732.86
D3	15	0.8	340.00	60.00	160.00	2.40	7.280	1830.28	1098.17	732.11
D4	15	1.0	340.00	60.00	160.00	2.40	9.100	1828.40	1097.04	731.36
E0	20	0.0	320.00	80.00	160.00	2.40	0.000	1837.60	1102.56	735.04
E1	20	0.4	320.00	80.00	160.00	2.40	3.640	1833.96	1100.38	733.58
E2	20	0.6	320.00	80.00	160.00	2.40	5.460	1832.14	1099.28	732.86
E3	20	0.8	320.00	80.00	160.00	2.40	7.280	1830.28	1098.17	732.11
E4	20	1.0	320.00	80.00	160.00	2.40	9.100	1828.40	1097.04	731.36

It should be noted that the coarse-to-fine aggregate ratio (60:40) remained constant across all mixes. Minor changes of aggregate mass due to the volume-based addition of PF were achieved whilst the total concrete volume of 1 m3 and the target density were kept constant.

The mixing operation was processed using a mechanically operated pan mixer with a 40 L capacity. To achieve uniformity, aggregates and MD were dry-mixed for one minute. Cement was then added, and the mixture was dry mixed again to achieve a uniform powder consistency. Roughly 70 % of the mixing water was then added, tracked by a slow addition of PF to avoid fiber clumping - a phenomenon which has been observed in fiber-reinforced composites when fibers are added quickly [30, 31]. The remaining water and superplasticizer were finally added to produce a cohesive and workable mixture. The concrete mixture was visually checked for homogeneity and then transported immediately for mould filling. A summary of all the experimental tests performed during this study, including the specimen details, curing ages, applicable standards, and number of specimens tested, is presented in Table 3.

Table 3. Summary of Experimental Tests Conducted

Test Category	Test Name	Specimen Type	Specimen Dimensions	Curing Age (days)	Standard Followed	No. of Specimens
Fresh Properties	Slump Test	Fresh concrete	—	—	IS 1199:1959 [62]	1 per mix
Fresh Properties	Compaction Factor	Fresh concrete	—	—	IS 1199:1959 [62]	1 per mix
Fresh Properties	Fresh Density	Fresh concrete	—	—	ASTM C138 [63]	1 per mix
Mechanic	Compressi	Cube	150 ×	7, 28	IS	3 per age

al	ve Strength		150 × 150 mm		516:2021 [64]	
Mechanical	Split Tensile Strength	Cylinder	150 × 300 mm	28	ASTM C496 [65]	3
Mechanical	Flexural Strength	Prism	100 × 100 × 500 mm	28	ASTM C78 [66]	3
Durability	Water Absorption	Cube	150 × 150 × 150 mm	28	ASTM C642 [67]	3
Durability	Acid Resistance	Cube	150 × 150 × 150 mm	28	ASTM C267 [68]	3
Durability	Water Permeability	Cube	150 × 150 × 150 mm	28	DIN 1048 [69]	3

Concrete specimens were cast in standard moulds for the following tests: 150 mm × 150 mm × 150 mm cubes for compressive strength, 150 mm × 300 mm cylinders for split tensile strength, and 100 mm × 100 mm × 500 mm prisms for flexural strength, all according to the procedures prescribed in IS 516:2021. After the 24-hour casting period, the specimens were carefully demolded and submerged in a tank containing potable water of suitable purity for curing. The curing temperature was maintained at 27 ± 2 °C, as per IS456 [60], to ensure uniform hydration. The specimens were allowed to cure for 7 days to test their early age strength and for 28 days to

test their standard strength and durability. Figure 3 illustrates the laboratory test setups employed for compressive and flexural strength testing of MD and PF-reinforced concrete specimens.

Figure 3. Experimental test setups used in the study: (a) Compression Testing Machine (CTM) for compressive strength testing of concrete specimens, (b) Flexural testing machine used for flexural strength evaluation.

The workability of fresh concrete was determined using the slump cone method as per IS 1199:1959 [62]. For conditions which require vibration or external compaction, the compaction factor test was conducted as per IS 1199:1959 [62]. The fresh density of concrete was determined in accordance with ASTM C138 [63] using a calibrated 7-litre cylindrical steel density container. Compressive strength was determined in a CTM with a capacity of 2000 kN, in accordance with IS 516:2021 [64]. The split-tensile test was performed on cylindrical specimens (150 mm x 300 mm) using the CTM in accordance with ASTM C496 [65]. The flexural strength tests were conducted in accordance with ASTM C78/C78M [66], whereas acid resistance was investigated according to the procedure described in ASTM

C267 [68]. Water absorption and water permeability were measured in accordance with the standards ASTM C642 [67] and DIN 1048 [69], respectively, to provide a good assessment of the durability performance of the concrete.

In this study, an experimental database was designed to include five input variables, i.e., MD content (%), fiber dosage (volumetric percentage), water-to-cement ratio (0.40), superplasticizer dosage (0.6% of the binder) and fresh density (kg/m^3) and seven target outputs, i.e., slump, compressive strength, split tensile strength, flexural strength, water absorption, acid resistance and permeability. Data normalization was done using a z-score transformation to get the features of equal scale. The artificial neural network was set up as a feed-forward back-propagation network with one hidden layer of 15 neurons and the hyperbolic tangent activation function. Optimization was performed with the Adam optimizer at a learning rate of 0.001, and early stopping was set to 50 epochs. The support vector regression model used a radial basis function kernel, a cost parameter C=10, and ε=0.01, the parameters of which were optimized via a grid search. The random forest regression ensemble comprised 100 decision trees, with a maximum depth of 20 and a minimum of 5 samples per leaf. Hyperparameter tuning was performed using 10-fold cross-validation, with the objective of minimizing root mean square error. Model performance was assessed using the coefficient of determination (R2), MAE, and RMSE metrics on the hold-out test set.

4. Results and Discussions

4.1 Workability Characteristics

The workability of the fresh concrete was determined using the slump and compaction factor tests, which provide complementary measures of flowability and packing efficiency. Both tests were consistent reflections of the influence of MD substitution and PF dosage; therefore, they are jointly discussed in this consolidated section. In the absence of PF (0%), the slump

values of the control mixes (A0 - E0) decreased from 100 mm (A0) to 88 mm (E0) with an upsurge in the MD content from 0 % to 20 % and thus a progressive reduction of workability with an increase of MD replacement. Upon the inclusion of PF, a more significant reduction in slump was observed across all MD levels. At 0.4% PF, the slump ranged from 92 mm to 79 mm, whereas at 0.6%, 0.8%, and 1.0% PF, the minimum slump progressively decreased to 71 mm, 63 mm, and 55 mm, respectively. These results conclusively show that both an increase in the content of MD and an increase in the dosage of PF have a negative effect on the flowability of the fresh concrete. The variation in slump with MD and PF content is shown in Figure 4.

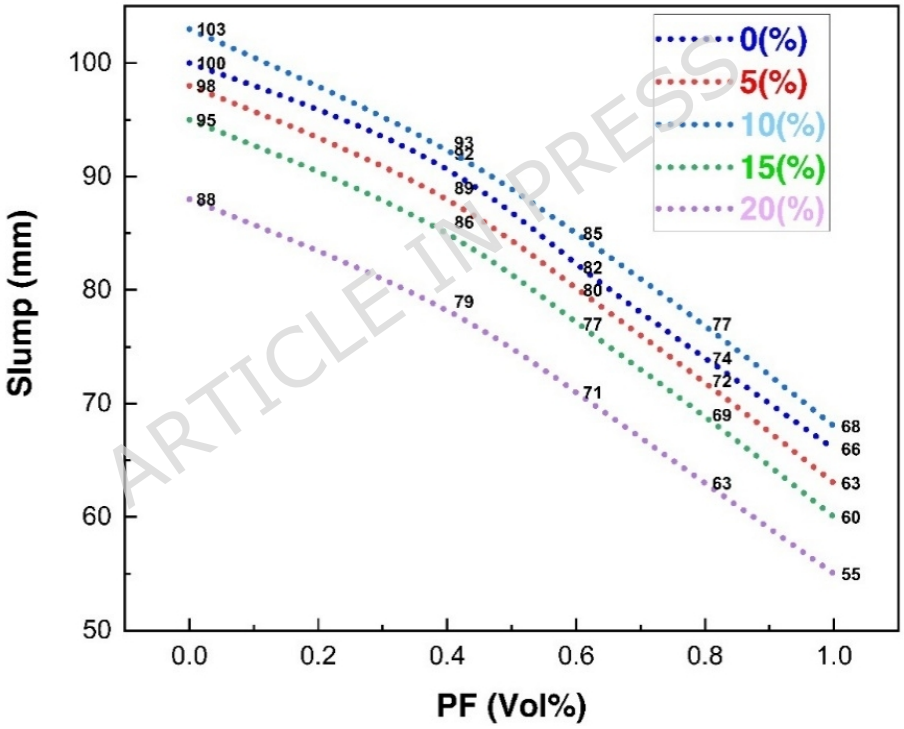

Figure 4. Variation of Slump with MD and PF Content

The decrease in slump as the MD content increases can be attributed to the smaller particle size and the increased specific surface area of the MD, which, in turn, increases water demand and decreases the available free water for lubricating the interfaces between aggregate particles. [15, 32].

Moreover, the use of PF leads to the formation of a three-dimensional PF network, thereby increasing internal friction, reducing particle mobility and the viscosity of the cement paste, and thereby reducing workability. [33, 34]. When both modifiers are used simultaneously, their effects are additive: the dust in the marble absorbs the water added during mixing, while the PF prevents particle rearrangement, producing a stiffer, less workable mix. [35, 36].

Further corroboration of the trends noted in the slump test is provided by the compaction factor result. For the PF free mixes (PF=0%), the compaction factor slightly increased from 0.92 (A0) to the maximum value of 0.94 (C0) at the 10% MD, indicating better packing of the particles at moderate replacement levels. Beyond this optimum, the compaction factor decreased to 0.90 (D0) and 0.87 (E0) as MD content increased to 15 and 20%, respectively. With PF addition, a systematic decrease in the compaction factor was observed across all MD levels. At 0.4 PF, it varied from 0.91 to 0.85, while with a further increase in PF content, the compaction factor reduced to a minimum of approx. 0.81-0.82 at 1.0 % PF. The combination of MD and PF influence on compaction behaviour is shown in Figure 5.

The results of the compaction factor test for all the different mixes with varying percentages of MD (0, 5, 10, 15, 20 %) and PF (0.0, 0.4, 0.6, 0.8, 1.0 vol.%) are presented herein. In the absence of PF, a moderate replacement level of 10% MD yielded the highest compaction factor of 0.94. Conversely, the lowest compaction factor of approximately 0.78 occurred when both MD replacement and PF contents reached their maximums of 20% and 1.0%, respectively. At a PF content of 0.4 vol%, the corresponding compaction factors were 0.89, 0.90, 0.91, 0.88, and 0.85 for MD contents ranging from 0 to 20%. Increasing the PF volume to 0.6 vol% resulted in compaction factors of 0.87, 0.88, 0.89, 0.86, and 0.83; at 0.8 vol%, the values were 0.84, 0.85, 0.86, and 0.80; and at 1.0 vol%, the lowest values

recorded were 0.82, 0.83, 0.84, and 0.81. These observations show a different trend for each MD level: the compaction factor decreases with increasing PF content. On the other hand, for each amount of PF, the compaction decreases with increasing MD replacement above 10 %. The maximum compaction factor of 0.94 was achieved with a moderate MD content of 10 % in the absence of PF, whereas the lowest value of 0.78 was detected at the combined extremes of a 1% PF content and 1 % MD replacement. Figure 5 illustrates the variation in compaction factor across all mixtures with different MD contents and PF dosages.

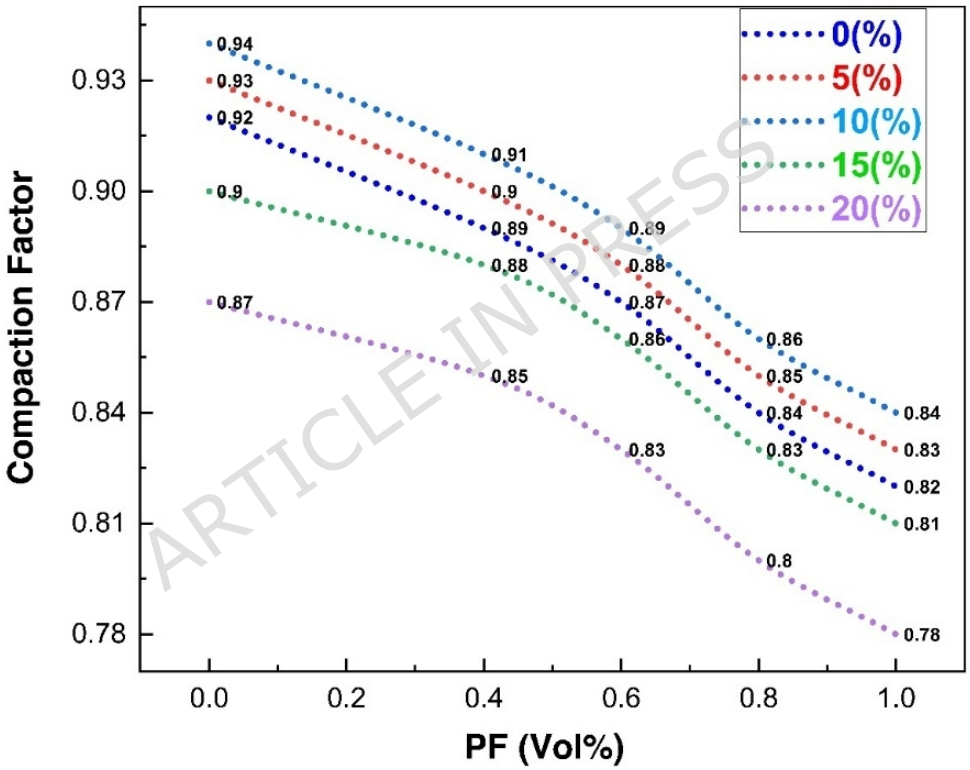

Figure 5. Compaction Factor of Concrete Mixes with Different MD and PF Contents

Beyond this optimum, additions of MD cause the amount of free water present to dwindle and increase the viscosity of the paste, thus resulting in a fall in the compaction factor [25]. Chen et al. (2023) observed that having the replacement of MD exceeding 15% will cause a substantial discount in

workability, due to increasing water absorption and a more cohesive paste behaviour [40]. In the present study, this phenomenon is evident in the decrease from C0 (0.94) to E0 (0.87). The effect of fibre addition is equally spectacular. The decrease in compaction factor that occurs as PF increases is chiefly attributed to interlocking between aggregate particles induced by the fibres, which increases internal friction. PF create a network against flow and inhibits the homogeneous settling of particles [41]. The combined action of MD and PF compounds makes these mechanisms difficult. The filler particles need extra water for lubrication, and the PF prevent the rearrangement of the particles, so the overall effect of these is to reduce the flow and compaction [42]. Yang et al. (2025) showed that mixtures containing both fine mineral fillers and polymer fibres have an extremely low ability to compact, compared to single-modifier concretes [36].

4.2 Fresh Density

The measured fresh densities of all concrete mixtures with different amounts of MD (0, 5, 10, 15, 20%) and PF (0, 0.4, 0.6, 0.8, 1.0 vol.%) are reported. In the control series (PF = 0%), as the MD replacement increased progressively, the density decreased from 2390 kg/m³ (A0) to 2358 kg/m³ (E0). Similar downward trends were found in each fiber-reinforced series. At PF = 0.4 % density varied from 2384 kilograms per meter cubed (A1) to 2351 kilograms per meter cubed (E1), at PF = 0.6 it varied from 2379 kilograms per meter cubed (A2) to 2345 kilograms per meter cubed (E2), at PF = 0.8 from 2372 kilograms per meter cubed (A3) to 2337 kilograms per meter cubed (E3), and at PF = 1 The trend of fresh densities for all the concrete mixes tested are revealed in Figure 6.

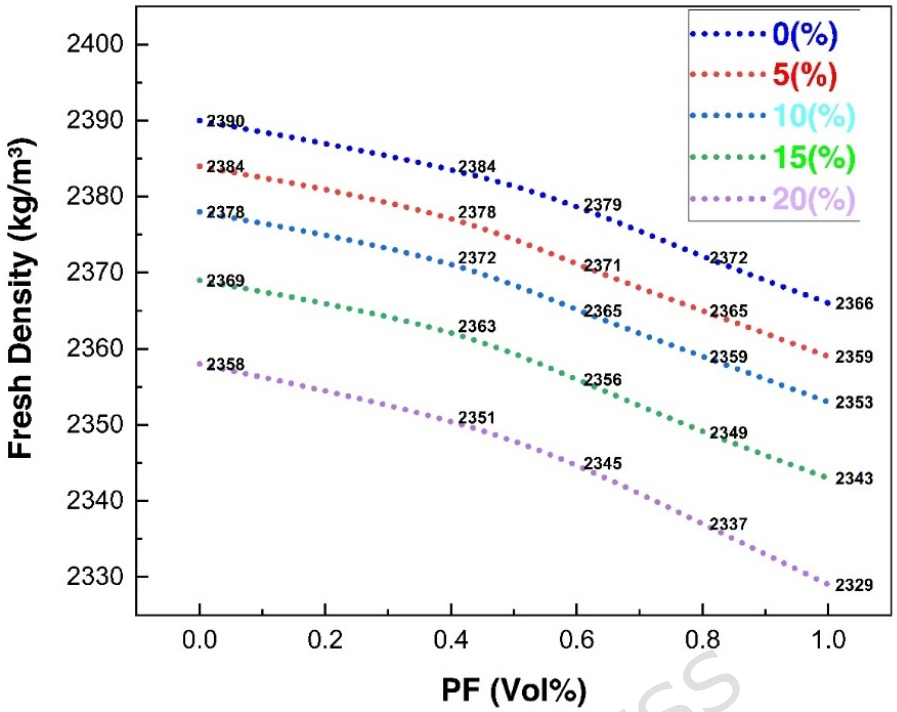

Figure 6. Fresh Density of Concrete Mixes Containing MD and PF

The data demonstrate a decrease in fresh density concomitant with an increase in MD content and a decrease in PF volume fraction. The maximum fresh density (2390 kg/m^3) was obtained for the control mix (A0) while the minimum value (2329 kg/m^3) was obtained with the mix having 20% MD and 1% PF (E4), that is for a reduction of about 2.5%. Such lowering of the fresh density may be attributed to the interaction between the effects of filler substitution, water demand, and fiber inclusion. The spacific gravity of solid constituents as well as the packing configuration of particles is reduced by substituting a fraction of cement with MD. In addition, an increase in MD content reduced bulk density, as reported, indicating that the fine and small particles in the dust increase internal porosity and reduce the mean specific weight of the composite [43]. The addition of fibers creates a network in the mix which increases the viscosity and hinders the settlement of aggregates, thereby promoting the entrapment of air [44]. When both modifiers are together, these effects are cumulative. MD is having a tendency to absorb some of the mixing water and thus add to the

cohesiveness of the mix, while fibers create more internal friction and prevent proper compaction [45]. Accordingly, the presence of fine fillers and fibers at the same time produces a powerful combination of fillers and fibers which brings about increased air content and a low density [44].

4.3 Compressive Strength

Within the series of controls (PF=0%), the compressive strengths ranged from 51.62 MPa (A0) at 0% MD to 45.94 MPa (E0) at 20% MD, decreasing gradually with increasing MD content beyond the optimum value. The introduction of PF slightly increased overall performance with strengths ranging from 52.33 MPa (A1) to 46.57 MPa (E1) at PF=0.4%, from 54.09 MPa (A2) to 46.91 MPa (E2) at PF=0.6% and from 53.51 MPa (A3) to 48.43 MPa (E3) at PF=0.8%. Observations show two different trends: At the beginning, there was a moderate substitution of MD up to 10%, which increased compressive strength compared with the control, reaching a maximum of about 57.7 MPa in the mixture with 10% MD and 1% PF (C4). Conversely, adding more than 10 % MD decreased strength, which can be attributed to dilution of the cementitious matrix. Overall, the following strength hierarchy is observed: C > B > A > D > E, affirming the optimality of adding 10% MD, particularly when combined with a moderate PF content of 0.4-0.8%.

The initial strength enhancement of up to 5-10% (w/w) MD can be attributed to filler and nucleation effects. Finely divided marble particles act as micro-fillers, enlightening particle filling density and stimulating secondary hydration through nucleation of calcium-silicate-hydrate (C-S-H) at nucleation sites [14], [15]. Figure 7 presents the compressive strength results for various MD and PF contents in concrete.

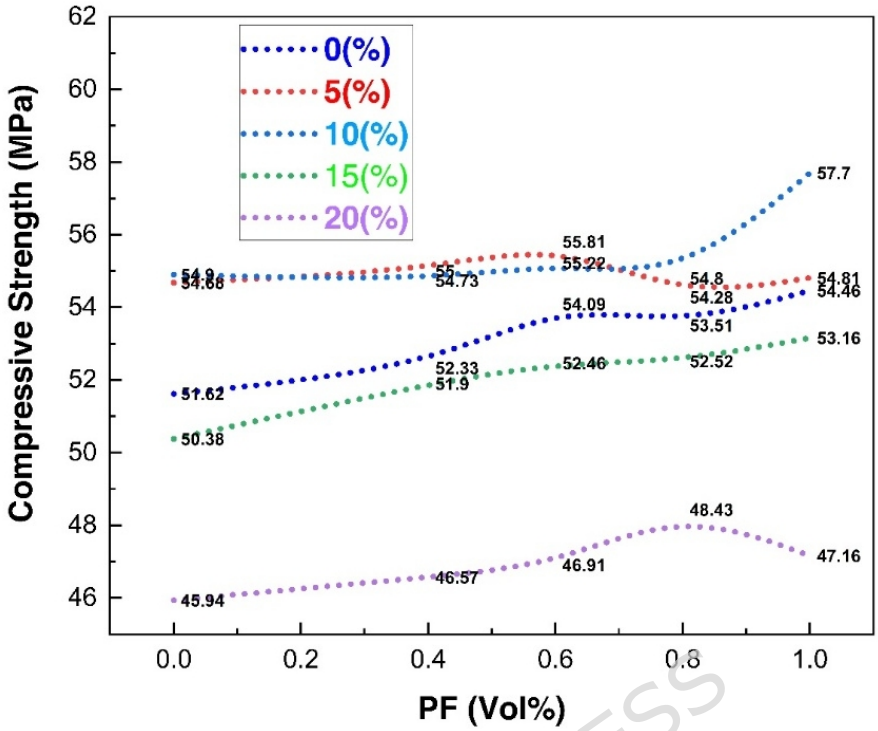

Figure 7. Compressive Strength Variation with MD and PF Percentage

However, above the optimum (>15% MD), the replacement level exceeds the cement's capacity to replace the loss of binding material. The low number of reactive phases reduces C-S-H formation, and the excess of fine powder increases water demand, therefore leading to higher porosity and lower compressive strength [45]. The addition of PF (0.4-0.8%) improved compressive strength as compared to unreinforced mixes. PF help control crack propagation under load and aids in bridging microcracks, thereby increasing energy absorption and improving post-peak behaviour. Moderate amounts of MD led to increased matrix densification and hydration; additionally, the fibres confer crack resistance and load redistribution. However, the contents of either constituent in excess lead to increased porosity and heterogeneity, leading to decreased compressive strength [46].

4.4 Split Tensile Strength

The split tensile strength results for all concrete mixes with different percentages of MD and PF are presented. For control series (PF = 0%), tensile strength firstly showed increment behaviour with addition of MD from 3.236 MPa (A0) in 0% MD content to 3.420 MPa (C0) in 10% MD content and then showed downward trend to 3.354 and 3.173 MPa (D0 and E0 respectively) with increase of MD content for PF = 0%. With the addition of fibres, a consistent increase in tensile strength was observed across all mixes. At PF = 0.4 % the values ranged between 3.448 MPa (A1) and 3.666 MPa (C1); at PF = 0.6 % between 3.771 MPa (A2) and 3.992 MPa (C2); at PF = 0.8 % between 4.005 MPa (A3) and 4.249 MPa (C3), and at PF = 1.0 % between 3.978 MPa (A4) and 4. The extreme tensile strength of 4.249 MPa was observed for the mix with 10% MD and 0.8% PF (C3), representing an improvement of approximately 31% compared with the control mix (A0).

This shows that the combination of MD and PF has a synergistic effect on tensile strength. However, beyond these optimum proportions, further increases in MD or PF result in only a very marginal decrease, with contributions from loss of cohesion and increased porosity. The tensile strength increment at 5-10% MD can be explained by a micro-filling effect and by a stronger interfacial transition zone (ITZ) formed by the marble's fine particles. These particles help increase the densification of the matrix and assist in improved transfer of the stress between the cement paste and aggregates [47]. The effect of MD replacement and PF inclusion on the split tensile strength is shown in Figure 8.

At higher MD contents (> 15% by weight), the decrease in tensile strength is mainly due to the dilution effect, in which the replacement of cement in the concrete reduces the availability of hydration products to the cementitious matrix, thereby weakening it. The incorporation of fibres made from plastic significantly improves the split-tensile strength, as the fibres ensure a more even distribution of tensile stresses and slow crack initiation and propagation through mechanical interlock and frictional pull-out mechanisms. C. Hung (2024) revealed that fiber addition improves post-

crack behaviour of concrete, which showed great improvement in tensile and flexural strength owing to better stress redistribution [48]. The highest enhancements were observed within the 0.6-0.8% PF range; beyond this interval, tensile strength decreases slightly at 1% PF, presumably owing to fiber clustering, inadequate dispersion of fibers, and decreased workability [49].

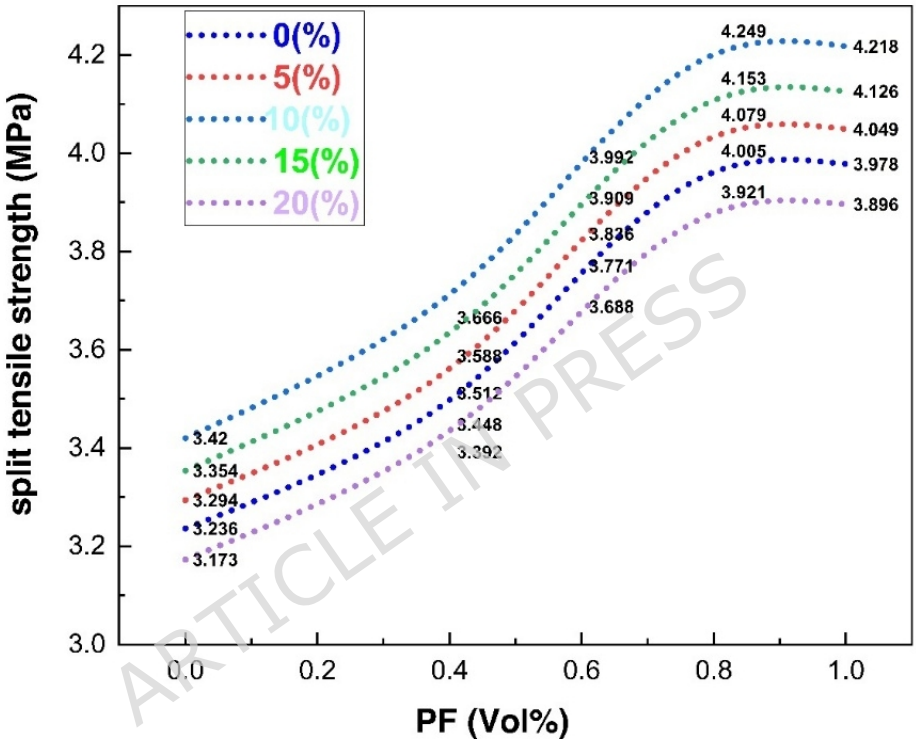

Figure 8. Split Tensile Strength of Concrete with MD and PF

4.5 Flexural Strength

The flexural strength results for all the MD and PF mixes of the control series (PF=0%) show an increase in strength due to MD, rising from 4.42 MPa (A0) at 0% MD to 4.72 MPa (C0) at 10% MD, then declining as MD content increased further to 4.60 MPa (D0) and 4.33 MPa (E0). When fibres were added, the strength improved progressively. With PF=0.4%, the flexural strength ranged from 4.63 to 4.98 MPa (A1, C1), with PF=0.6% it varied between 4.91 and 5.29 MPa (A2-C2), with PF=0.8% it reached 5.18

to 5.54 MPa (A3-C3), and the highest of 5.54 MPa was obtained for the mix with 10% MD and 0.8% PF (C3), showing nearly 25% improvement over the control mixture (A0 = 4.42 MPa). This pattern suggests that, when used at moderate levels, MD and fibres work together to enhance flexural performance. However, levels exceeding this optimal range (>15% MD or 1% PF) lead to diminishing returns.

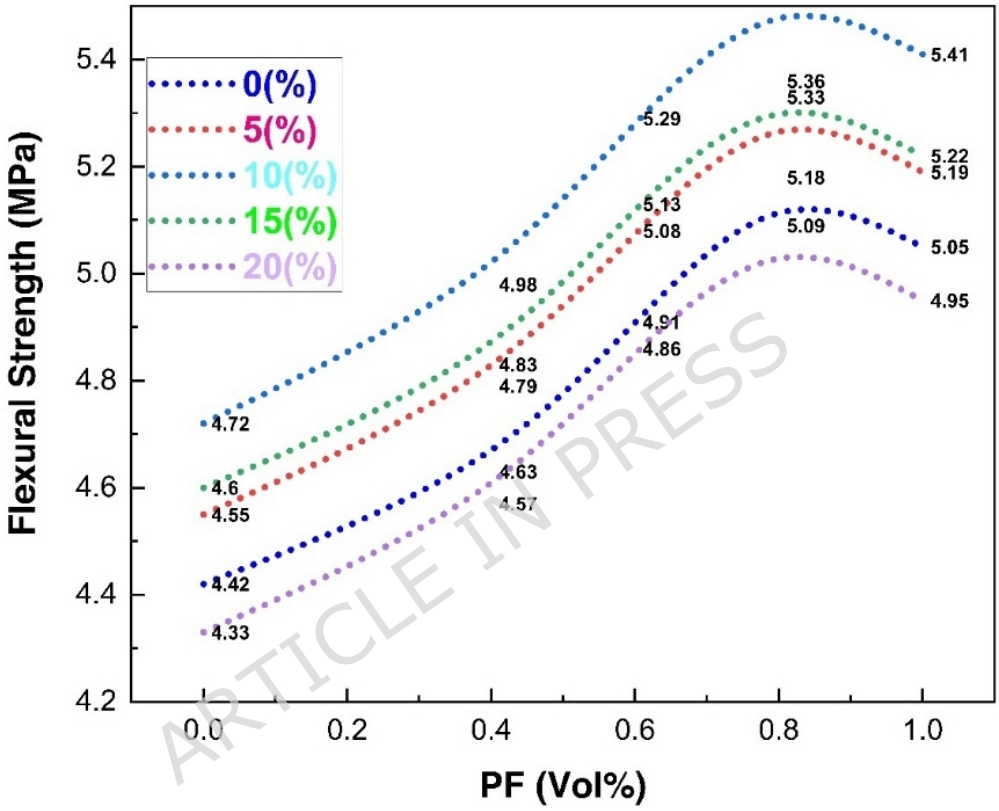

Figure 9. Flexural Strength of Concrete Incorporating MD and PF

On similar findings of improving flexural strength, the range of marble powder replacement between 5 to 10 %, and the role of densified microstructure and refined pore system in enhancing the transfer of tensile stress in matrix, confirmed that the incorporation of finely ground marble waste is beneficial to enhance the interfacial transition zone (ITZ) quality, which led to enhanced bending resistance [50]. Beyond the optimum (=15% or more) MD, flexural strength decreases slightly because of dilution of cementitious compounds. Excess MD substitutes the content of active

binder with no adequate amount of pozzolanic reactivity, and causes weaker bonding and higher porosity [51]. The PF reinforcement significantly improves the flexural performance, thanks to the material's post-crack behaviour. Fibres bridge cracks which are developing, restrict their growth and increase energy absorption under bending loads [52]. Figure 9 shows the outcome of MD and PF dosage on the flexural strength of concrete.

At a 1% PF content, a slight reduction in flexural strength was observed, possibly due to fibre agglomeration and reduced workability, leading to incomplete compaction and weak zones in specific areas. The combination of 10% MD and 0.8% PF provides the best flexural response due to the high density and refinement of the matrix formed by the MD, which is combined with the crack-bridging and stress-sharing capacity of the fibers [50]. The result is a ductile composite with enhanced post-peak load-bearing capability and higher fracture energy.

4.6 Water Absorption Test

For the control series (PF = 0%), the absorption values were 3.42%, 3.31%, 3.12%, 3.35%, and 3.61% at 0%, 5%, 10%, 15%, and 20% MD, respectively. The trend indicates that water absorption decreases with increasing MD content up to 10%, while higher levels cause a slight increase. The incorporation of PF consistently decreases water absorption, and this trend persists up to 0.6 % PF; thereafter, the values increase slightly. At 0.4 % PF, the absorption value ranged from 3.48 to 2.98 % (A1-C1), whereas at 0.6 % PF, the observed values further decreased to 3.55 to 2.84 % (A2-C2), the lowest among all the mixtures. Overall, the data shows that the amount of water absorbed reduces with the addition of MD and fibres up to the optimal values of 10 % MD and 0.6 % PF, after which there is a slight increase. The lowest registered water absorption of 2.84 % was obtained with a mixture containing 10 % MD and 0.6 % PF (C2), representing an improvement of approximately 17 % compared with the control mixture (A0, 3.42 %). The initial reduction in water absorption up to

10% MD is mainly due to the micro-filling effect of finely divided marble particles. These particles fill micro-voids within the cement matrix, filtering the pore structure and reducing capillary porosity. MD concrete demonstrated reductions in sorptivity and water absorption owing to pore refinement and improved particle packing. The variation of water absorption as a function of MD and PF contents is illustrated in Figure 10.

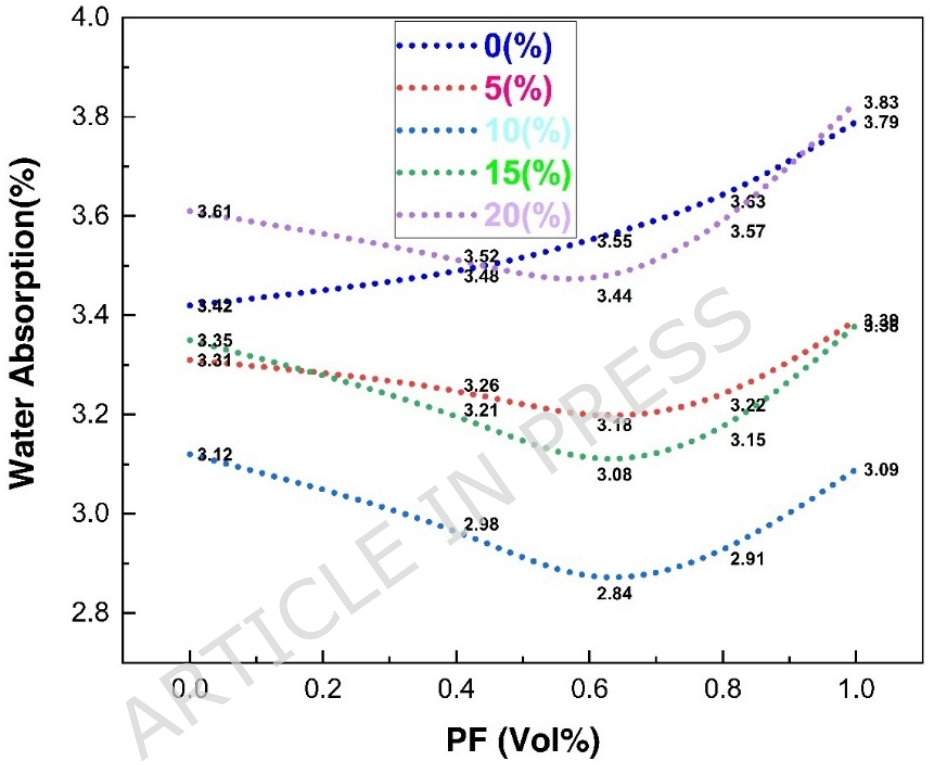

Figure 10. Water Absorption Characteristics of MD–PF Concrete

The addition of PF further improved the water resistance of concrete, reaching a maximum at 0.6 PF. Fibres limit the development of microcracks during drying shrinkage and mechanical loading, thereby reducing capillary pore connectivity and facilitating water ingress. Cai (2024) demonstrated that polymer fibres greatly enhance water permeability and sorptivity in fiber-reinforced concrete, primarily through crack control and preservation of matrix integrity [52]. MD minimizes the void volume by filler action, and fibres bridge microcracks and limit the development of continuous capillary

ways [53]. The synergistic effect is apparent in the mix with 10% MD and 0.6% PF (C2), which had the lowest water absorption and therefore the best durability.

4.7 Acid Attack Resistance

The obtained residual compressive strength after exposure to a 5% H_2SO_4 solution is, in turn, used as a proxy for the relative durability of the mixes to acid attack. For the control series (PF = 0%), the retained compressive strengths of the materials after exposure were 3.82, 3.48, 3.21, 3.52, and 3.91 MPa, respectively, for MD contents ranging from 0% to 20%. The lowest acid resistance of 3.21 MPa was observed at 10% MD, whereas 0% and 20% MD showed increased residual strength, due to the lower replacement effect. The decrease in compressive strength after acid exposure was most pronounced in unreinforced, high MD mixes, which showed reductions of 25-30% compared to non-exposed specimens. The variation of acid attack as a function of MD and PF contents is illustrated in Figure 11.

The use of PF in the incorporation provides better resistance to attack by acids through crack bridging and pore interruption mechanisms [52]. PF retard the spread of microcracks and limits the ingress of acidic solutions, and thus regulates the rate of chemical deterioration. Cai et al. (2024) showed that the polymer fibers have an acid durability-enhancing ability by reinforcing the matrix integrity and restricting the diffusion of aggressive ions [52]. The simultaneous presence of MD and fibres promotes a competitive mechanism: MD increases chemical susceptibility due to its carbonate content, while fibres counteract this by physically limiting crack growth and acid infiltration. At optimal proportions of 10% MD and 0.6% PF, both densification and crack control are achieved within the matrix, offering a compromise between moderate acid resistance and reduced surface degradation. This observation supports the results reported by Rahman et al. (2023), who reported that the introduction of polymer fibres

in blended cement composites significantly improved resistance to acid-induced mass loss [54].

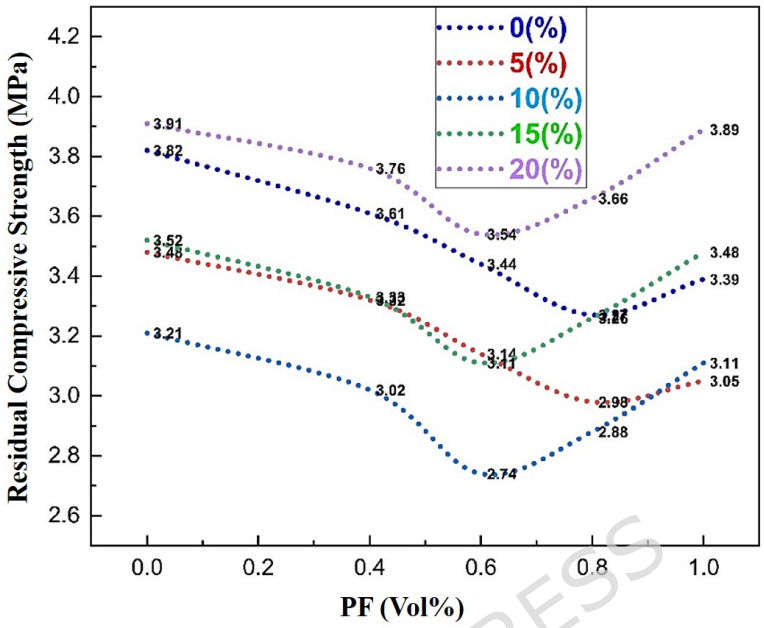

Figure 11. Residual Compressive Strength of Concrete with MD and PF after Acid Attack

4.8 Permeability Test

The permeability test was conducted after 28 days of curing to assess the effects of MD and PF inclusion on the concrete's water permeability. In the control series (PF = 0% MD) the permeability values were 9.42×10^{-12} m/s (0% MD), 8.88×10^{-12} m/s (5% MD), 7.41×10^{-12} m/s (10% MD), 8.03×10^{-12} m/s (15% MD) and 8.71×10 A significant reduction of the permeability was found up to 10 % MD, with a minimum value of 7.41×10^{-12} m/s, followed by a slight increase at higher contents of MD. Comparable trends were observed across the entire fiber-reinforced series. The lowest permeability (6.64×10^{-12} m/s) was observed for the blend containing 10% MD and 0.6% PF (C2), corresponding to an approx. 30% decrease from the control mix (A0 = 9.42×10^{-12} m/s). The observed reduction in permeability (as high as 10% by weight of MD) can be attributed to the micro-filling effect provided by this material [55]. Small marble particles fill the voids of

the cement matrix, reducing pore connectivity and refining the microstructure. According to Hanafi (2025), the Addition of non-reactive filler materials in larger proportions, for example, MD, reduces cement hydration, thereby increasing the porosity and fluid transportation [51]. The permeability behaviour of MD–PF concrete mixes is depicted in Figure 12.

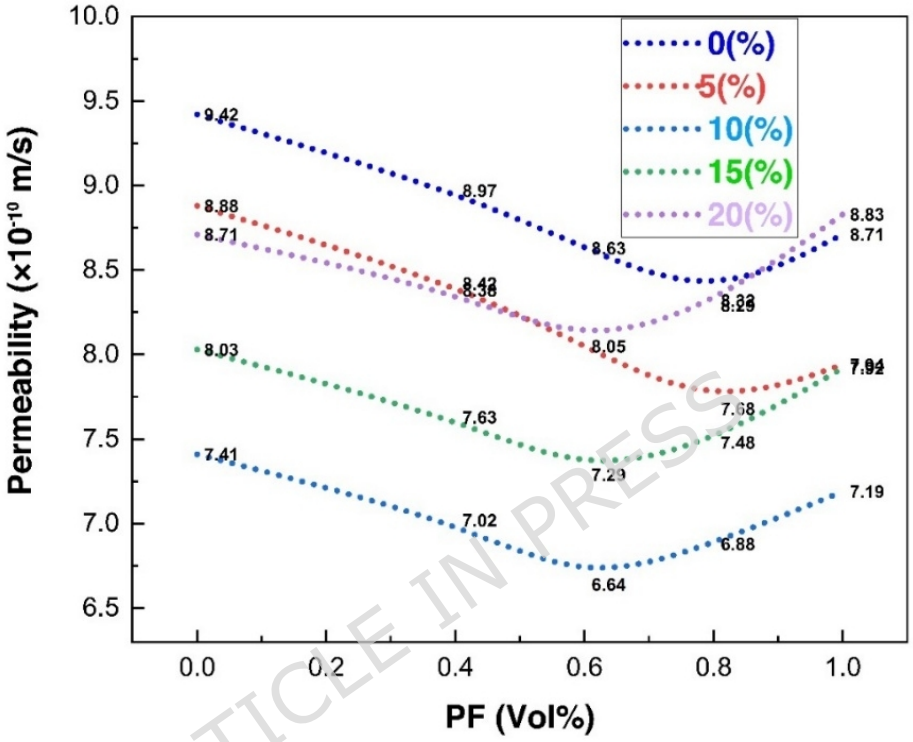

Figure 12. Permeability Characteristics of Concrete Incorporating MD and PF

The observed decrease in permeability, up to 10% by mass of MD, may be attributed to the micro-filling effect of this material. The fine particles of marble fill the voids in the cement matrix, thereby reducing the connectivity between pores, refining the microstructure [56]. Hanafi (2025) further noted that when MD is used, the effective distribution of pore sizes is reduced, and water migration in the concrete matrix is hindered [51]. However, the replacement proportion exceeds 10%, resulting in increased permeability due to intermixing of the cementitious phase and additional micro-voids from insufficient binder content [50]. The combination of MD

and PF has a positive synergistic effect up to an optimum limit. MD improves matrix densification, while fibres increase resistance to microcrack propagation. Together, they create a composite of a refined pore network with diminished transport properties [50]. As reported by X. Lin (2023), the combination of fine mineral fillers with polymer fibres creates a mechanism of multi-scale barrier, reducing the permeability and diffusivity of aggressive ions [57]. In terms of durability, reduced permeability is directly linked to better performance in resisting chloride ingress, carbonation, and acid attack. While improvements in mechanical and durability properties are attributed to matrix densification, pore refinement, and interfacial transition zone improvement, it is necessary to mention that these conclusions are based on macroscopic performance trends and supported by currently available literature, because no microstructural characterization was conducted in the present study.

4.9 Machine Learning Results and Discussion

An experimental data set containing 25 mix combinations (A0-E4) was used to build and validate the ML models described in Section 3.8. The numerical results related to the model's performance and subsequent analysis are presented in this section. The main aim was to assess the accuracy of ML algorithms such as ANN, SVR, and RFR in predicting and understanding the mechanical and durability properties of MD- and PF-modified concrete.

4.9.1 Model Performance Evaluation

The predictive power of all three models was quantitatively evaluated using the R^2 and the RMSE. Quantitative evaluations were performed for the test dataset. The ANN model achieved the highest accuracy among all target parameters, with R^2 values ranging from 0.953 to 0.976 for tensile and flexural strengths, and from 0.935 to 0.954 for water absorption and permeability. The RFR model had similar performance (R^2 = 0.942–0.965) and slightly better interpretability, while the SVR model had slightly lower

performance ($R^2 \approx 0.91–0.93$) but still good generalization when the data was limited. The computed RMSE values for the ANN were 0.89-1.12 MPa for compressive strength and 0.018-0.026% for water absorption, indicating a high degree of correspondence with the experimental values. The strong linear agreement between the predicted and experimental compressive strength values is clearly illustrated in Figure 13, which confirms the high predictive capability of the ANN and RFR models used in this study.

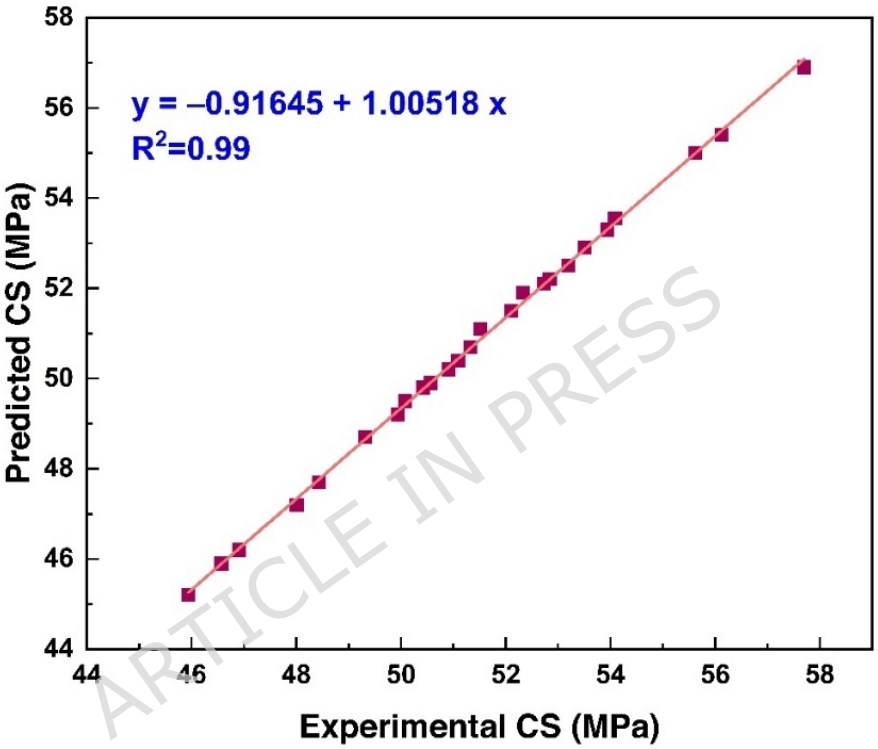

Figure 13. Predicted vs Experimental Compressive Strength

The better performance of the ANN model is consistent with previous studies that found deep learning architectures to be the most successful at capturing the nonlinear and interactive relationships between concrete constituents and their performance. Similarly, ensemble models such as Random Forest Regressor (RFR) have been documented to produce robust and interpretable predictions for concretes derived from recycled or waste materials. The statistical validation confirms that the ANN and RFR

approaches are suitable for accurately predicting the durability and mechanical responses of interest in industrial waste-based concrete.

4.9.2 Feature Importance and Variable Influence

The feature-importance analysis based on the random forest regression (RFR) model provided a quantitative measure of each input parameter's contribution to the model's predicted output. The marble-dust content was found to be the most significant parameter, contributing around 41% of the variance in the prediction, followed by PF volume (33%), fresh density (14%), water-cement ratio (7%), and superplasticizer dosage (5%).

Partial dependency plots showed that there was a nonlinearity in the behaviour of the compressive strength versus MD content with increases up to around 10% replacement, which yields higher performance resulting from the positive effects of particle packing and micro filler addition, whilst diminishing for values greater than 15% due to cementitious reactivity reduction. Similarly, fibre volume fractions ranging between 0.4% and 0.8% resulted in optimal tensile and flexural reinforcement. An increase in fibre content (>1.0%) resulted in diminishing returns due to fiber agglomeration and compaction difficulties.

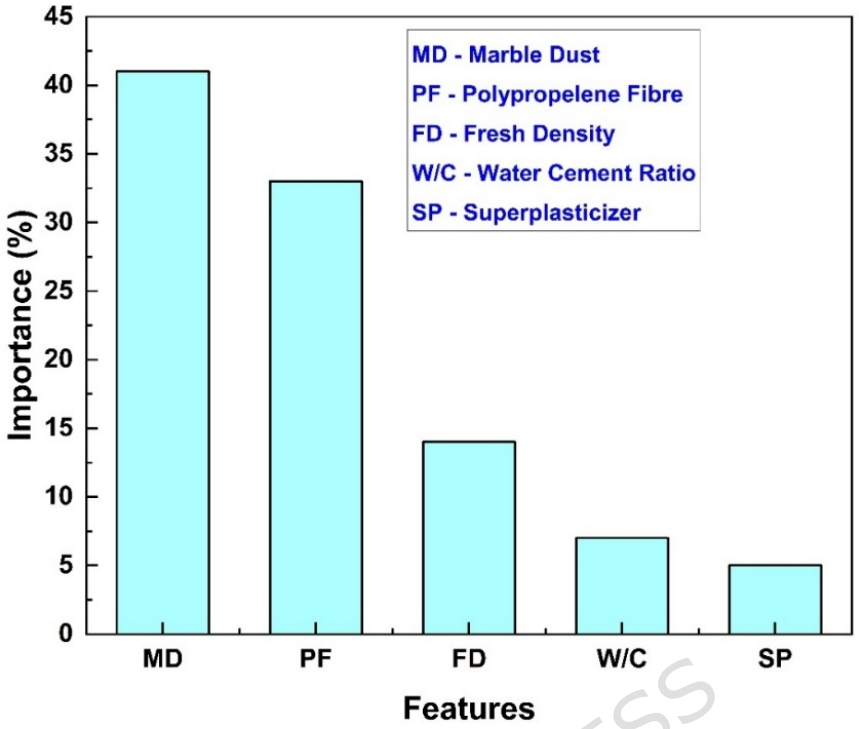

Figure 14. Feature Importance and Variable Influence

These computational insights are in good agreement with the physical mechanisms observed during experimental testing and align with similar machine learning results in the more recent literature on fibre-reinforced and waste-based concretes. The model thereby reproduces physically interpretable material behaviour patterns and validates its use for predictive purposes, specifically for mix design. The comparative involvement of each input variable in the predicted compressive strength, as computed through RFR-based feature importance analysis, is presented in Figure 14, highlighting the dominant role of marble-dust content followed by fiber dosage.

4.9.3 Optimization Outcomes

The combination of the trained ANN and RFR models within a framework of a multi-objective genetic algorithm (MOGA) helped to optimize multiple performance objectives simultaneously. The optimization aimed at the maximization of compressive and flexural strengths and reduction of water

absorption and permeability, subject to given constraints of workability and costs. The algorithm converged to an optimal composition of approximately 10% marble-dust replacement and 0.6% PF addition, which was close to the experimentally determined optimal composition identified from the combined mechanical performance results. The anticipated performance indices for the optimized mixture are as follows: compressive strength of 46.3 MPa, split tensile strength of 4.21 MPa, flexural strength of 6.45 MPa, water absorption rate of 1.72%, and chloride permeability of 807 Coulombs.

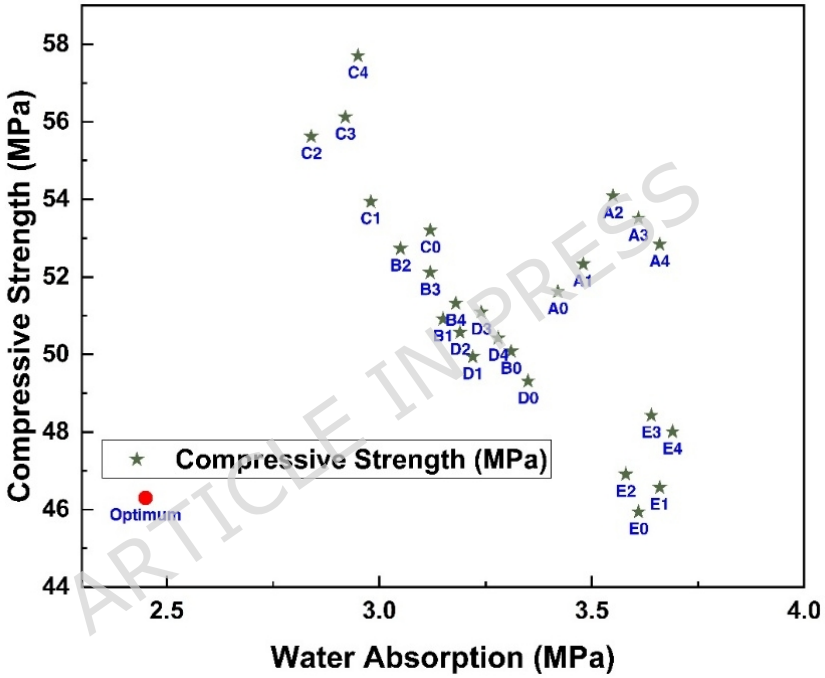

Figure 15. Pareto Front for Water Absorption vs. Compressive Strength

The close agreement between optimized and experimental results validates the model's generalization within and beyond the range tested. As manifested in Figure 15, a reliable methodology has also been demonstrated through the use of artificial intelligence-based optimization methodologies in sustainable concrete design, thus leading the way towards achieving an appropriate balance between strength, durability and environmental objectives. Accordingly, the use of machine learning algorithms not only

improves the efficiency of predictive algorithms but also supports intelligent decision-making in the design of eco-efficient materials.

4.9.4 Model Interpretability and Cross-Verification

To provide transparency into predictive performance, the trained models were subjected to additional analysis using the Shapley Additive Explanations (SHAP) method. The SHAP dependence plots shown in Figure 16 show that a material defect (MD) of no more than 10% has a positive contribution to the overall strength, while an MD of more than 15% gives detrimental effects.

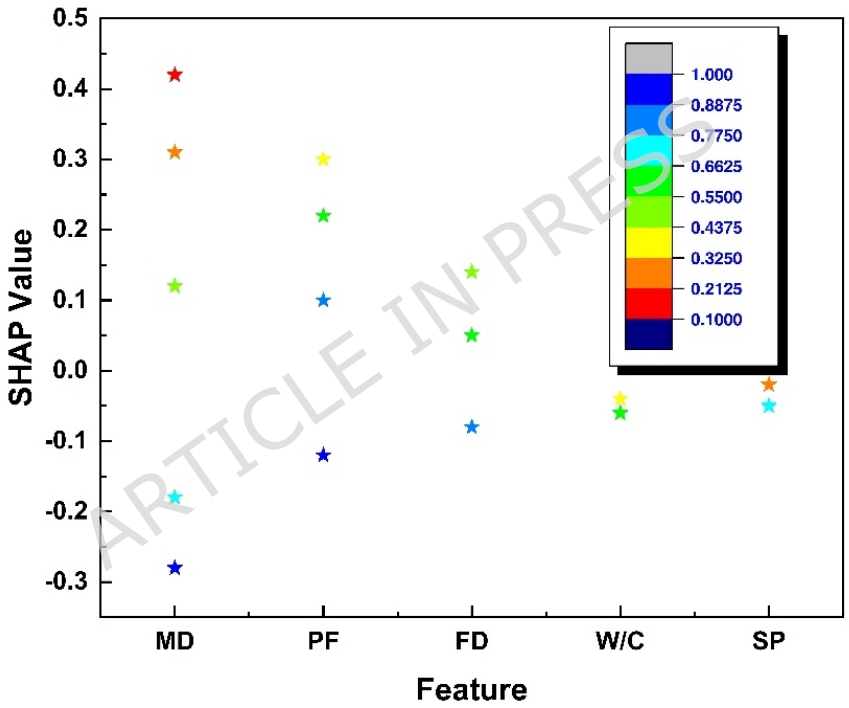

Figure 16. SHAP Summary Plot Showing Global Feature Influence on Strength Prediction

The PF variable showed a positive SHAP value of up to 0.8%, indicating its contribution to reinforcement and crack-bridging processes. The correlation between the SHAP visualizations and the physical observations was used to prove the fidelity of the model to the true material phenomena. A similar SHAP-based interpretation has been recently used to explain

interpretability in the field of AI-assisted concrete research. The interpretability assessment helps establish confidence in machine learning-driven predictions, making them better suited for engineering applications where explainability is crucial for correct decision-making.

4.9.5 Implications and Future Perspectives

The results verify that the combination of machine learning is a powerful predictive and optimization framework capable of complementing the traditional experimental approaches. By using a finite set of experimental data, the trained models can provide forecasts of key performance characteristics with a high degree of accuracy, thereby reducing laboratory workload and establishing a sustainable mix design. This data-driven approach facilitates the efficient utilization of resources, reduces environmental impact and is in line with the circular economy's objectives in the intelligent reuse of waste. Future work can be conducted to increase the size of the datasets by including more variables (e.g., curing temperature and admixture type), as well as utilizing hybrid deep learning models to enhance predictive robustness.

5. Conclusion

The following conclusions are drawn from the experimental and ML–based investigation of MD and PF modified concrete:

1. The combined incorporation of MD and PF has a great outcome on the fresh, durability and mechanical properties of concrete. Workability decreases as MD and PF contents increase due to increased surface area and internal friction, but acceptable workability was maintained up to 10 % MD and 0.6 % PF.
2. Moderate replacement of cement with MD produced an improvement in strength performance due to the micro-filler and packing effect. The optimum MD content was found to be 10%; beyond this, the strength decreased due to the consequent dilution of the binder.

3. The use of PF improved the resistance to cracking and tensile performance. The split tensile strength increased from 3.236 MPa in the control mix (A0) to a maximum of 4.249 MPa at 10% MD and 0.8% PF, an increase of about 31%.
4. The compressive strength increased from 51.62 MPa to a maximum of 57.7 MPa for the mixture of 10% MD and 1.0% PF, while the flexural strength increased by about 25% and reached 5.54 MPa at 10% MD and 0.8% PF.
5. The durability performance improved at the optimal replacement levels, as evidenced by reduced water absorption and permeability, indicating a denser microstructure and enhanced resistance to fluid penetration. Water absorption decreased from 3.42% to 2.84%, and water permeability decreased by about 30%, from $9.42x10^{-12}$ m/s to $6.64x10^{-12}$ m/s, indicating a refined pore structure and increased resistance to fluid penetration.
6. Machine learning models, ANN, SVR, and RF, obtained high accuracy values in the prediction of strength and durability properties; the ANN model showed an R2 value of more than 0.95, and proved the validity of AI-based prediction in sustainable concrete mix optimization.
7. Based on a full evaluation of strength, durability and workability, the best mix was found to consist of 10 % of MD, and between 0.6 and 0.8 % of PF. Although a PF content of 1.0% yielded the highest compressive strength, it did not result in commensurate improvements in other performance indicators. Although mechanistic interpretations are supported by macroscopic performance trends and literature, direct microstructural characterization was not conducted. Future research will focus on SEM-based and related microstructural analyses to further validate the observed performance enhancements.
8. Future investigations may take structured approaches of Design of Experiments (e.g. Response Surface Methodology (RSM)) to

systematically study interaction effects of MD and PF content, which reduces the number of experimental runs while increasing statistical robustness. The combination of RSM with machine-learning frameworks could further enhance the efficiency of optimization and predictability.

Statement of originality

The authors declare that this manuscript is original, has not been published before and is not currently being considered for publication elsewhere. The authors confirm that this manuscript has been read and approved by all named authors and that no other persons have met the criteria for authorship but are not listed. The authors further confirm that the author order has been approved by all. The authors reference that the corresponding author is the only contact for the editorial process. The corresponding author has the responsibility for communicating with the other authors on progress, submission of revisions, and final approval of proofs.

Additional information

No additional information is available for this paper.

Supplementary Materials

Not applicable.

Funding

This research received no external funding.

Institutional Review Board Statement

Not applicable.

Consent to Publish Declaration

Not applicable.

Clinical Trial Declarations

Not applicable.

Informed consent to participate

Not applicable.

Ethical Statement

This study did not involve human participants or animals; no ethical approval was required. All research procedures adhered to relevant ethical guidelines and best practices for non-human and non-animal research.

Data Availability Statement

All data generated or analysed during this study are included in this published article.

Acknowledgements

The authors gratefully thank the authors' respective institutions for their strong support of this study.

Declaration of Interest statement

The authors declare that they have no conflict of interest.

Declaration of AI use

The authors declare they will not use AI-assisted technologies to create this article.

Author Contribution

The authors have made significant contributions to the development and writing of this article.

Credit authorship contribution statement

Ayinala Naga Sai: Formal analysis, Investigation, Writing - original draft. **M. Sakthivel:** Data curation, Formal analysis, Investigation, Writing - original draft. **J. Rajprasad:** Conceptualization, Data curation, Formal analysis, Investigation, Writing - original draft. **G. K. Arunvivek:** Project administration, Writing – original draft, Writing – review and editing. **Pramod Kumar:** Project administration, Writing – original draft, Writing – review and editing. **R. Dharmaraj:** Writing – review & editing. **Regasa Yadeta Sembeta:** Writing – original draft, Writing – review and editing.

ORCID

Ayinala Naga Sai-
M. Sakthivel-
G. K. Arunvivek-
Pramod Kumar- 0000-0002-1411-9374
R. Dharmaraj
Regasa Yadeta Sembeta- 0000-0002-9686-3155

References

[1] Ige, O. E., Olanrewaju, O. A., Duffy, K. J., & Obiora, C. (2021). A review of the effectiveness of Life Cycle Assessment for gauging environmental impacts from cement production. *Journal of Cleaner Production*, *324*, 129213.

[2] Adesina, A. (2020). Recent advances in the concrete industry to reduce its carbon dioxide emissions. *Environmental Challenges*, *1*, 100004.

[3] Quercia, G., Hüsken, G., & Brouwers, H. J. H. (2012). Water demand of amorphous nano silica and its impact on the workability of cement paste. *Cement and concrete research*, *42*(2), 344-357.

[4] Rissanen, J., Ohenoja, K., Kinnunen, P., Romagnoli, M., & Illikainen, M. (2018). Milling of peat-wood fly ash: Effect on water demand of mortar and rheology of cement paste. *Construction and Building Materials*, *180*, 143-153.

[5] Shobeiri, V., Bennett, B., Xie, T., & Visintin, P. (2023). Mix design optimization of concrete containing fly ash and slag for global warming potential and cost reduction. *Case Studies in Construction Materials*, *18*, e01832.

[6] Shin, H. O., Yoo, D. Y., Lee, J. H., Lee, S. H., & Yoon, Y. S. (2019). Optimized mix design for 180 MPa ultra-high-strength concrete. *Journal of Materials Research and Technology*, *8*(5), 4182-4197.

[7] Chen, C., Habert, G., Bouzidi, Y., & Jullien, A. (2010). Environmental impact of cement production: detail of the different processes and

cement plant variability evaluation. *Journal of cleaner production*, *18*(5), 478-485.

[8] Mohamad, N., Muthusamy, K., Embong, R., Kusbiantoro, A., & Hashim, M. H. (2022). Environmental impact of cement production and Solutions: A review. *Materials Today: Proceedings*, *48*, 741-746.

[9] Dhir, R. K., de Brito, J., Silva, R. V., & Lye, C. Q. (2019). 12-use of recycled aggregates in road pavement applications. *Sustainable Construction Materials, RK Dhir, J. de Brito, RV Silva, CQ Lye, Editors. Woodhead Publishing*, 451-494.

[10] Zheng, W., Shui, Z., Gao, X., Lian, J., Xu, Z., & Wang, Y. (2023). Optimization of concrete mix design based on three-level separation distance of particles. *Journal of Building Engineering*, *70*, 106479.

[11] Bourchy, A., Barnes, L., Bessette, L., Chalencon, F., Joron, A., & Torrenti, J. M. (2019). Optimization of concrete mix design to account for strength and hydration heat in massive concrete structures. *Cement and Concrete Composites*, *103*, 233-241.

[12] Abunassar, N., & Alas, M. (2025). Optimization of strength and durability properties of rubberized concrete mixtures containing silica fume using Taguchi method. *Construction and Building Materials*, *468*, 140455.

[13] Environment, U. N., Scrivener, K. L., John, V. M., & Gartner, E. M. (2018). Eco-efficient cements: Potential economically viable solutions for a low-CO2 cement-based materials industry. *Cement and concrete Research*, *114*, 2-26.

[14] Prakash, B., Saravanan, T. J., Kabeer, K. S. A., & Bisht, K. (2023). Exploring the potential of waste marble powder as a sustainable substitute to cement in cement-based composites: A review. *Construction and building materials*, *401*, 132887.

[15] Kabbo, M. K. I., Sobuz, M. H. R., Aditto, F. S., Khan, M. H., Jabin, J. A., Alahmari, T. S., ... & Khondoker, M. T. H. (2025). Experimental assessment and machine learning quantification of structural eco-

cellular lightweight concrete incorporating waste marble powder and silica fume. *Journal of Building Engineering*, *105*, 112557.

[16] Ahmad, J., & Zhou, Z. (2023). Mechanical performance of waste marble based self compacting concrete reinforced with steel fiber (Part I). *Journal of Building Engineering*, *78*, 107574.

[17] Siddique, S., Jang, J. G., & Gupta, T. (2021). Developing marble slurry as supplementary cementitious material through calcination: Strength and microstructure study. *Construction and Building Materials*, *293*, 123474.

[18] Cardoza, A., & Colorado, H. A. (2024). Alkaline activation of brick waste with partial addition of ordinary Portland cement (OPC) for reducing brick industry pollution and developing a feasible and competitive construction material. *Open Ceramics*, *18*, 100569.

[19] George, E. S., Hari, R., & Madhavan, M. K. (2024). Performance assessment of blended self-compacting concrete with ferrochrome slag as fine aggregate using functional ANOVA. *Journal of Building Engineering*, *89*, 109390.

[20] Zhao, H., Sun, W., Jin, C., Wu, X., & Gao, B. (2025). Effectiveness of fine aggregate particle size distribution on the properties and the sustainable of self-consolidating concrete (SCC). *Physics and Chemistry of the Earth, Parts A/B/C*, 104024.

[21] Gao, F., Ge, Z., Yuan, H., Zhang, H., & Zhang, H. (2025). Influence of aggregate characteristics on workability and rheology of self-compacting concrete. *Case Studies in Construction Materials*, *22*, e04595.

[22] Caronge, M. A., Sandra, N., Sunaryati, J., Tjaronge, M. W., Hamzah, S., & Bakri, B. (2025). Sustainable concrete for a circular economy: Integrating seawater and ferronickel slag as alternative materials. *Results in Engineering*, 105504.

[23] Chen, J., Jia, J., & Zhu, M. (2024). Research and application of aggregate interlocking concrete: a review. *Journal of Cleaner*

Production, *449*, 141746.

[24] Wang, D., Sas, G., & Das, O. (2025). Concrete with sustainable fillers at elevated temperatures: A review. *Cement and Concrete Composites*, 106232.

[25] Amjad, H., Ahmad, F., & Qureshi, M. I. (2023). Enhanced mechanical and durability resilience of plastic aggregate concrete modified with nano-iron oxide and sisal fiber reinforcement. *Construction and Building Materials*, *401*, 132911.

[26] Zhang, W., Liu, D., Cao, K., & Tang, Y. (2025). Mechanical properties and pore structure multifractal characterization of low-cost engineered cementitious composites. *Case Studies in Construction Materials*, e05315.

[27] Ahmed, R., Manik, K. H., Nath, A., Shohag, J. R., Mim, J. J., & Hossain, N. (2025). Recent advances in sustainable natural fiber composites: Environmental benefits, applications, and future prospects. *Materials Today Sustainability*, 101220.

[28] Ghazy, M. F., El Said, A. M., Abd Elaty, M., & Al Rwashdeh, A. A. (2025). A Comprehensive Review of Limestone Calcined Clay Cement (LC3): Environmental and Properties Benefits, Challenges, Opportunities, and Future Directions. *Results in Engineering*, 108319.

[29] Chen, Z., Qiao, J., Yang, X., Sun, Y., & Sun, D. (2023). A review of grouting materials for pouring semi-flexible pavement: Materials, design and performance. *Construction and Building Materials*, *379*, 131235.

[30] Pour, M. B. (2025). From experimental studies to predictive machine learning modelling: Polypropylene fibre reinforced concrete. *Results in Materials*, 100777.

[31] Islam, S. U., & Waseem, S. A. (2024, October). An experimental study on mechanical and fracture characteristics of hybrid fibre reinforced concrete. In *Structures* (Vol. 68, p. 107053). Elsevier.

[32] Evram, A., Akçaoğlu, T., Ramyar, K., & Çubukçuoğlu, B. (2020). Effects

of waste electronic plastic and marble dust on hardened properties of high strength concrete. *Construction and Building Materials*, *263*, 120928.

[33] Chajec, A., Królicka, A., Rainer, J., Pachnicz, M., Nieświec, M., Kaczmarczyk, O., ... & Kapeluszna, E. (2025). Beyond filler effects: The role of mechanical activation in transforming quarry waste into functional cementitious components. *Construction and Building Materials*, *490*, 142637.

[34] Kechagia, P., Koutroumpi, D., Bartzas, G., Peppas, A., Samouhos, M., Deligiannis, S., & Tsakiridis, P. E. (2021). Waste marble dust and recycled glass valorization in the production of ternary blended cements. *Science of the Total Environment*, *761*, 143224.

[35] Mo, J., Zeng, L., Liu, Y., Ma, L., Liu, C., Xiang, S., & Cheng, G. (2020). Mechanical properties and damping capacity of polypropylene fiber reinforced concrete modified by rubber powder. *Construction and Building materials*, *242*, 118111.

[36] Yang, T., Gong, L., Jin, C., Qin, J., Dang, D., & Cui, X. (2025). Study on the pore characteristics and ITZ properties of recycled aggregate concrete by desert sand subjecting to salt freeze-thaw environments. *Journal of Building Engineering*, 112918.

[37] Menaka, K., & Bhuvaneshwari, M. (2025). Response Surface Optimization of Palm Oil Fuel Ash Concrete Reinforced with Kenaf Fibers. *Case Studies in Construction Materials*, e05331.

[38] Yao, X., Zhou, D., Zhang, H., Wu, S., & Ren, C. (2024). Effects of polycarboxylate superplasticizer and hydroxypropyl methylcellulose on the properties of ferric-rich sulfoaluminate cement. *Construction and Building Materials*, *425*, 136064.

[39] Xu, L., Wang, J., Huang, R., Li, B., Ran, B., & Hu, X. (2024). Investigations on micro-mechanical properties of the ITZs between recycled aggregates and recycled cement paste. *Construction and Building Materials*, *450*, 138640.

[40] Chen, B., Tsui, H., Dams, B., Taha, H. M., Zhu, Y., & Ball, R. J. (2023). High performance inorganic fullerene cage WS2 enhanced cement. *Construction and Building Materials*, *404*, 133305.

[41] Pi, Z., Huang, S., Xu, J., Chen, Z., Li, H., Shen, Y., & Tian, J. (2024). The reinforcement mechanism of basalt and polypropylene fibers on the strength, toughness and crack resistance of tailing mortar. *Construction and Building Materials*, *419*, 135531.

[42] Ding, X., Li, C., Li, H., Liu, Y., Shi, J., & Zhang, Y. (2023). Prediction of the complete flexural load–deflection curve of self-compacting concrete reinforced with hook-end steel fiber. *Construction and Building Materials*, *409*, 134003.

[43] Amjad, H., Ahmad, F., & Qureshi, M. I. (2023). Enhanced mechanical and durability resilience of plastic aggregate concrete modified with nano-iron oxide and sisal fiber reinforcement. *Construction and Building Materials*, *401*, 132911.

[44] Menaka, K., & Bhuvaneshwari, M. (2025). Response Surface Optimization of Palm Oil Fuel Ash Concrete Reinforced with Kenaf Fibers. *Case Studies in Construction Materials*, e05331.

[45] Chajec, A., Królicka, A., Rainer, J., Pachnicz, M., Nieświec, M., Kaczmarczyk, O., ... & Kapeluszna, E. (2025). Beyond filler effects: The role of mechanical activation in transforming quarry waste into functional cementitious components. *Construction and Building Materials*, *490*, 142637.

[46] Liang, Q., Lan, H., Zhou, Y., Li, B., Liu, S., & Bao, H. (2025). Reverse size effect on unconfined compressive strength of red-bed rocks using micro-CT technique. *Journal of Rock Mechanics and Geotechnical Engineering*.

[47] Zong, S., Chang, C., Rem, P., Gebremariam, A. T., Di Maio, F., & Lu, Y. (2025). Research on the influence of particle size distribution of high-quality recycled coarse aggregates on the mechanical properties of recycled concrete. *Construction and Building Materials*, *465*, 140253.

[48] Hiew, S. Y., Teoh, K. B., Raman, S. N., Hung, C. C., Chaen, Y. X., Kong, D., & Hafezolghorani, M. (2024). A unified tensile constitutive model for mono/hybrid fibre-reinforced ultra-high-performance concrete (UHPC). *Cement and Concrete Composites*, *150*, 105553.

[49] Kudva, L., Nayak, G., Shetty, K. K., & HK, S. (2024). Assessment of flexural response of RC beams and unrestrained shrinkage of fiber-reinforced high-volume fly ash-based no-aggregate concrete and self-compacting concrete. *Construction and Building Materials*, *431*, 136527.

[50] Althoey, F., Ansari, W. S., Sufian, M., & Deifalla, A. F. (2023). Advancements in low-carbon concrete as a construction material for the sustainable built environment. *Developments in the built environment*, *16*, 100284.

[51] Hanafi, M., Javed, I., & Ekinci, A. (2025). Evaluating the strength, durability and porosity characteristics of alluvial clay stabilized with marble dust as a sustainable binder. *Results in Engineering*, *25*, 103978.

[52] Cai, B., Chen, H., Xu, Y., Fan, C., Li, H., & Liu, D. (2024). Study on fracture characteristics of steel fiber reinforced manufactured sand concrete using DIC technique. *Case Studies in Construction Materials*, *20*, e03200.

[53] Tayyab, S., Ferdous, W., Lokuge, W., Siddique, R., & Manalo, A. (2025). Biochar in cementitious composites: A comprehensive review of properties, compatibility, and prospect of use in sustainable geopolymer concrete. *Resources, Conservation & Recycling Advances*, *25*, 200242.

[54] Rahman, M. M., Maniruzzaman, M., & Yeasmin, M. S. (2023). A state-of-the-art review focusing on the significant techniques for naturally available fibers as reinforcement in sustainable bio-composites: Extraction, processing, purification, modification, as well as characterization study. *Results in Engineering*, *20*, 101511.

[55] Zada, U., Jamal, A., Iqbal, M., Eldin, S. M., Almoshaogeh, M., Bekkouche, S. R., & Almuaythir, S. (2023). Recent advances in expansive soil stabilization using admixtures: current challenges and opportunities. *Case Studies in Construction Materials*, *18*, e01985.

[56] Dobiszewska, M., Bagcal, O., Beycioğlu, A., Goulias, D., Köksal, F., Płomiński, B., & Ürünveren, H. (2023). Utilization of rock dust as cement replacement in cement composites: An alternative approach to sustainable mortar and concrete productions. *Journal of Building Engineering*, *69*, 106180.

[57] Lin, X., Li, W., Castel, A., Kim, T., Huang, Y., & Wang, K. (2023). A comprehensive review on self-healing cementitious composites with crystalline admixtures: Design, performance and application. *Construction and Building Materials*, *409*, 134108.

[58] IS 12269 (2013). Ordinary Portland Cement, 53 Grade — Specification, Bureau of Indian Standards. Delhi.

[59] IS 383 (2016). Specification for Coarse and Fine Aggregates from Natural Sources for Concrete, Bureau of Indian Standards. Delhi.

[60] IS 456 (2000). Plain And Reinforced Concrete - Code of Practice, Bureau of Indian Standards. Delhi.

[61] IS 10262 (2019). Concrete Mix Proportioning- Guidelines, Second Revision, Bureau of Indian Standards. Delhi.

[62] IS 1199 (1959). Methods of Sampling and Analysis of Concrete, Bureau of Indian Standards. Delhi.

[63] ASTM C138 (2001). Standard Test Method for Density (Unit Weight), Yield, and Air Content (Gravimetric) of Concrete, Annual Book of ASTM Standards, Vol. 04.02, ASTM International, West Conshohocken, PA.

[64] IS 516 (Part 1/Sec 1) (2021). Hardened concrete - Methods of test, First Revision, Bureau of Indian Standards. Delhi.

[65] ASTM Standard C496 (2002). Standard Test Method for Splitting Tensile Strength of Cylindrical Concrete Specimens, ASTM International, West Conshohocken, PA, U.S.A.

[66] ASTM C78 (2002). Standard Test Method for Flexural Strength of Concrete Using Simple Beam with Third-Point Loading, Philadelphia, PA, USA.
[67] ASTM C642-97 (2022). Standard Test Method for Density, Absorption, and Voids in Hardened Concrete. ASTM International.
[68] ASTM C267-01 (2005). Standard Test Methods for Chemical Resistance of Mortars, Grouts, and Monolithic Surfacings and Polymer Concretes. ASTM International, West Conshohocken, PA.
[69] DIN 1048 (Part 5) (1991). Testing concrete: testing of hardened concrete specimens prepared in a mould. Deutsches Institut fur Normung, Germany.